14

Advanced Medical Imaging and Reverse Engineering Technologies in Craniometric Study

Supakit Rooppakhun[1], Nattapon Chantarapanich[2] and Kriskrai Sitthiseripratip[3]
[1]*School of Mechanical Engineering, Suranaree University of Technology*
[2]*Institute of Biomedical Engineering, Prince of Songkla University*
[3]*National Metal and Materials Technology Center (MTEC)*
Thailand

1. Introduction

In crime scenes and accidents, the standard operating protocols for personal identification is not difficult when the entire body is found. As a result, the investigators can directly collect the sample of the decrease such as facial photograph, DNA, fingerprint and dental record in order to compare to possible relatives or with ante-mortem profile (De Valck, 2006). However, the investigators are not always lucky. In severe accidents such aircraft crashes, only little information of the decrease is available, the skin and soft tissue may be completely burnt out and the skeleton can be broken into small pieces due to the impact. The skeleton examination in historical sites by archaeologists presents even more complication. The archaeologists need not only to identify general aspects of the skeleton, for instant age, sex, cause of death, stature and race, but also to estimate the period of death and the possibility to discover the particular person that might be significant in the history.
Several techniques have been applied to assist the identification of the decrease ranging from the simplest technique which may acquire the evidence from the personal belonging until using the advance scientific techniques. These techniques can be generally categorized into two methods, invasive and non-invasive. The invasive method includes biochemical analysis, microscopy, accelerator mass spectrometry radiocarbon dating (with standard C-14), ancient DNA analysis, histology and endoscope whereas the non-invasive technique involved the aid of engineering technologies such as radiographic analysis and computed tomography (CT) examination.
From 1975 – 2005, the archaeological researches had been increasingly conducted by means of non-invasive techniques which 112 of 245 researches have applied the non-invasive technique and the trend of investigation gradually moved from invasive to non-invasive examinations (Zweifel, et al., 2009). The first non-invasive technique has been presented to the public in 1896 which the radiographic analysis was used to examine the ibis mummy in Belgium (Van Tiggelen, 2004). Soon after that, archaeologist realized the importance of radiological technique and applied broadly to examine great numbers of mummy (Dedouit, et al., 2010; Friedrich, et al., 2010; Recheis, et al., 1999; Zweifel, et al., 2009). One main

advantage of radiography includes the ability to access general aspects of mummy without releasing the bandages which may be destroyed important features or contaminated. In the early 1900s, another non-invasive medical examination device, computed tomography scanner, has been invented by Alessandro Vallebona, but the technology has remained unpopular until the 1970s which modern era of computed tomography scanner began (Hill, 2009). Not too long, computed tomography scanner became an effective tool in examination the autopsy. The computed tomography generally relies on medical imaging processing combined with reverse engineering principles which the object is captured the profile and presented the virtual three-dimensional models in computer. With these advanced features, the perspective of archaeology and forensic medicine has changed into three-dimensional aspect. Consequently, The two-dimensional radiographic image occlusion and the problem such uncertainty from bias of investigator in direct measurements are eliminated.

Apart from the advantages of computed tomography in forensic medicine, it also becomes an effective clinical diagnosis device in many hospitals. The use of three-dimensional model allows the surgeon to examine the abnormality of organs in any configurations which the two-dimensional technique may be inaccessible. Moreover, the three-dimensional models can be used to simulate the surgical operation prior surgery (Fürnstahl, et al., 2010), subsequently reduce operating time and increase safety of patients. Alternative uses of computed tomography include morphometric study (Chantarapanich, et al., 2008; Mahaisavariya, et al., 2002) and the evaluation the risk of implant usage (Mahaisavariya, et al., 2004; Sitthiseripratip, et al., 2003)

The purpose of this chapter is to present and discuss the medical imaging and reverse engineering techniques by means of demonstrating the application in craniometric study. Obviously, recent craniometric studies have been employed by two-dimensional techniques or direct measurement (Steyn & Işcan, 1997; Deshmukh & Devershi, 2006; Dayal, et al, 2008; Sangvichien, et al., 2008; Matamala, et al, 2009) such as the use of spreading caliper, sliding vernier calliper, mandibulometer and standard flexible steel tape. The diverse mentioned measurement techniques reflect the lack of engineering aids which the current trend in forensic medicine need the advanced technologies to provide the accurate measurements. Therefore, the scope of demonstration includes the brief detail of reverse engineering as to provide for who may not familiar with, data acquisition technique using computed tomography scanner, measurement of skull anatomical parameters and sex determination method based on logistic function. By this way of demonstration, the overview of forensic medicine by aid of advance medical imaging and reverse engineering is obtained.

2. Reverse engineering

Reverse engineering has been widely applied several years in clinical fields and forensic medicine (Aamodt, et al., 1999; Aghayev, et al., 2008; Fürnstahl, et al., 2010). Initially, reverse engineering was first used in free-form product designs which the conventional "Forward Engineering" has limited drawing functions and time consumption. Product design based on "Forward Engineering", the process involves turning the conceptual product design to physical product whereas reverse engineering is inversed (Zhou & Xi, 2002).

The process of reverse engineering involves turning the physical product back to the virtual models (normally three-dimension) (Li, et al., 2002; Várady, et al., 1997). From the three-dimensional virtual models, the conceptual design can be obtained. Reverse engineering can be described as two phases which are digitization and reconstruction phase, as summarized

in Fig. 1. The digitization phase involves the data acquisition of the physical model using various types of scanner. The initial geometry from the scanner is then obtained in three forms, point clouds, polygon model and series of image depending on the acquisition technique of each scanner. In the reconstruction phase, the obtained data is processed in order to reconstruct the three-dimensional model. with "At this step, the elimination of noise data and filtering of unnecessary data may also be performed. For the production phases, it may be added as a final step in reverse engineering. This phase employs various manufacturing processes to fabricate the three-dimensional virtual model. However, this phase may not be mandatory, because sometime the geometry is only stored in database without any further processing.

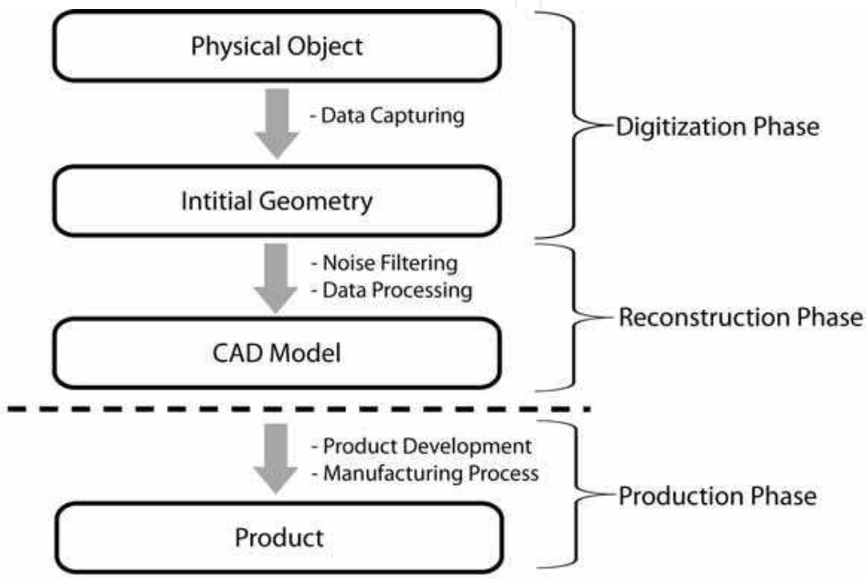

Fig. 1. Diagram of reverse engineering process.

The digitization methods can be categorized into two approaches which are tactile approach (contact method) and non-contact approach (Li, et al., 2002; Várady, et al., 1997). For tactile approach, the device contacts to the physical object directly whereas the non-contact approach uses the medium in digitization instead without contact of device.

The characteristic of tactile approach is relatively simple. Touch probe is used in conjunction with robotic mechanism such as coordinate measurement machine (CMM), articulated arm or computer numerical control (CNC) devices to determine the position of the object (Cartesian coordinate). The accuracy is considered to be a main advantage of tactile approach, nevertheless the digitization process is quite slow and difficult to digitize complex geometry. A wide range of object can be applied with this approach regardless of color, shininess and transparency, this approach is not appropriate for deformable materials.

In non-contact approach, the medium is used to measure the physical object using the principle of reflection or penetration. Laser beam and white light are medium sources commonly found in many three-dimensional scanners and they rely on the principle of reflection. The medium travels from the generator to the object before reflects and transmits to the receiver unit. The determination of geometry can be processed using at least one two-

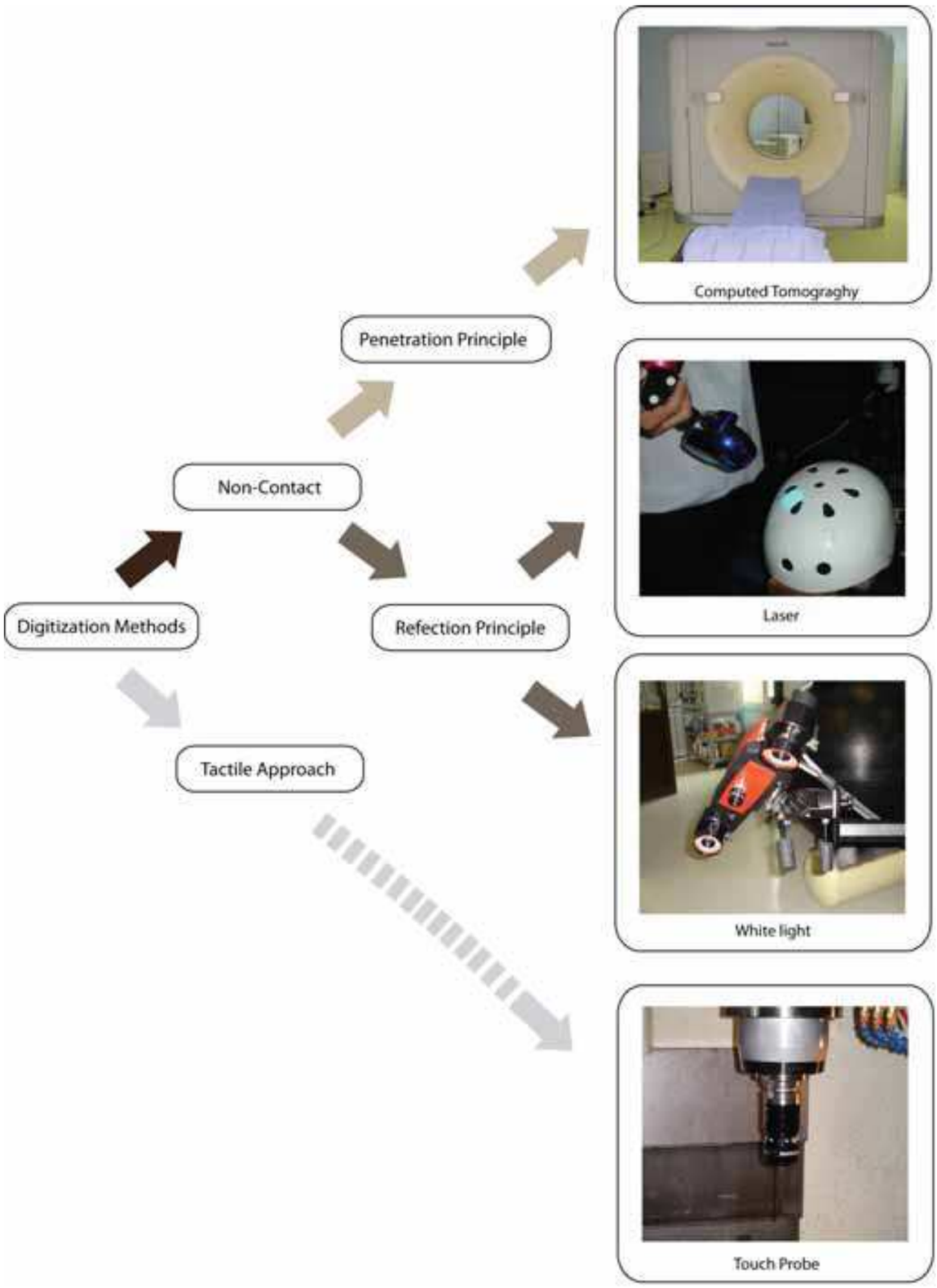

Fig. 2. Digitization Methods.

dimensional images combined with some optical parameters such as reflection angle, distance and time of flight. The initial geometry is presented in form of cloud point or of polygon model. Use of laser beam and white light has advantage in fast digitization and continuous data, but too shiny and transparent object present complication.

Even the laser beam and white light systems are applied in many forensic studies (Park, et al., 2006; Thali, et al., 2003; Vanezis, et al., 2000), but probably, the most efficient system for forensic studies is the use of non-contact device based on principle of penetration. This system uses the medium that can go though the object to capture both internal and external geometries. The most popular device is computed tomography scanner which involves the use of X-ray.

The digitization process initializes the transmission of the X-ray through the object. A set of data acquisitions is performed with the constant interval throughout entire object which subsequently give a series of slice image (Hounsfield, 1980). Each slice contains the information of object's position and the value of Hounsfield unit (HU). The density of object is proportional to the Hounsfield value. The higher Hounsfield value indicates high-density object such as enameled and cortical bone whereas the lower Hounsfield value indicates low-density object such as cancellous bone, fat and soft tissue. Various Hounsfield values of various substances are given in Table 1. In order to reconstruct the three-dimensional model, the optimal Hounsfield values must be selected (threshold). After that the threshold regions of each slice are combined to construct the volumetric model.

For the computed tomography device, the speed of digitization and ability to examine the internal topology are considered to be superior, but the artifact (noise data) caused by metallic structure is drawback.

Substances	Hounsfield values
Air	-1000
Fat	-70 to -90
Water	0
Tissue	+20 to +35
Blood Volume	Approx. +40
Bone	+900

Table 1. Hounsfield values of various substances. (Hounsfield, 1980)

3. Data acquisition of skull

Specimen of 104 dry cadaveric skulls donated by the Department of Anatomy, Faculty of Medicine, Khon Kaen University, Thailand is used to demonstrate the application of advanced medical imaging and reverse engineering technologies in craniometric study. The cadaver includes 63 males with average age of 55.16 years (standard deviation 18.38 years) and 41 females with average age of 49.00 years (standard deviation 17.94 years). The age rages from 17–81 years at the time of death. The skulls are placed in acrylic box with a set of four. The reverse engineering technique by means of spiral computed tomography scanner (Siemens AG, Germany) is used to capture the profile of each skull as shown in Fig. 3. The data acquisition protocol is axial scan with tube voltage of 120 kV and tube current of 100 mA. The digitization is performed with 1.5-mm slice thickness and the reconstruction is

done at 1-mm thickness. Each slice contains the volumetric data that represent the density and position (contour) of the skull. The computed tomography images are then processed with medical image processing software (Mimics, Materialise NV, Belgium). To begin the reconstruction of three-dimensional model, a proper Hounsfield value (normally +900 for bone structure) is selected. After that, the threshold regions are used to calculate the complete topology of three-dimensional skull. The reconstruction process of skull model is illustrated in Fig. 4.

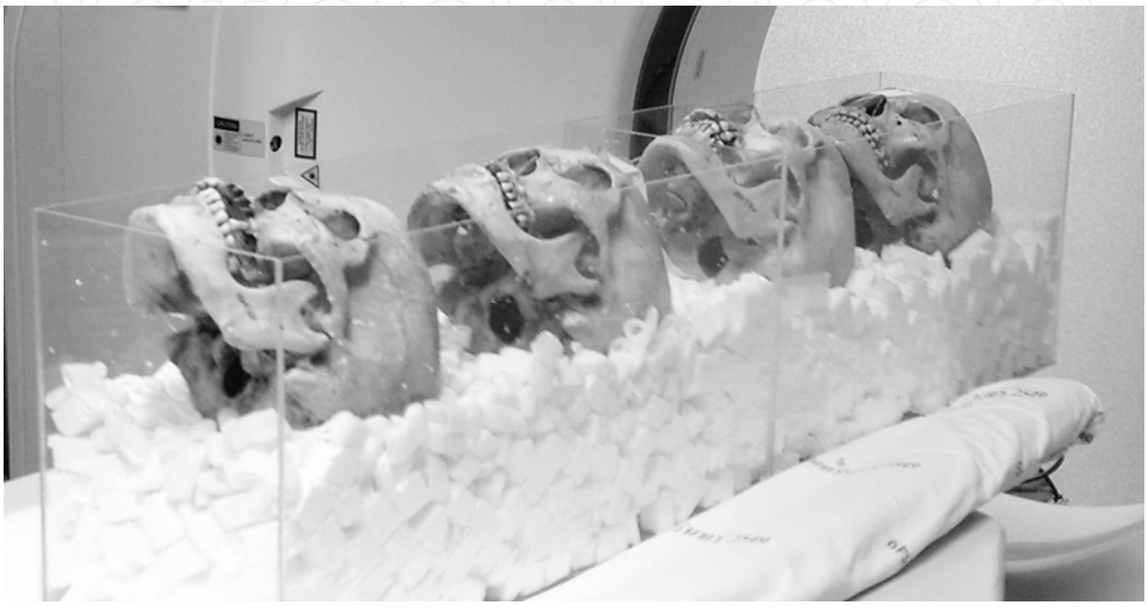

Fig. 3. A set of skull during data acquisition using computed tomography scanner.

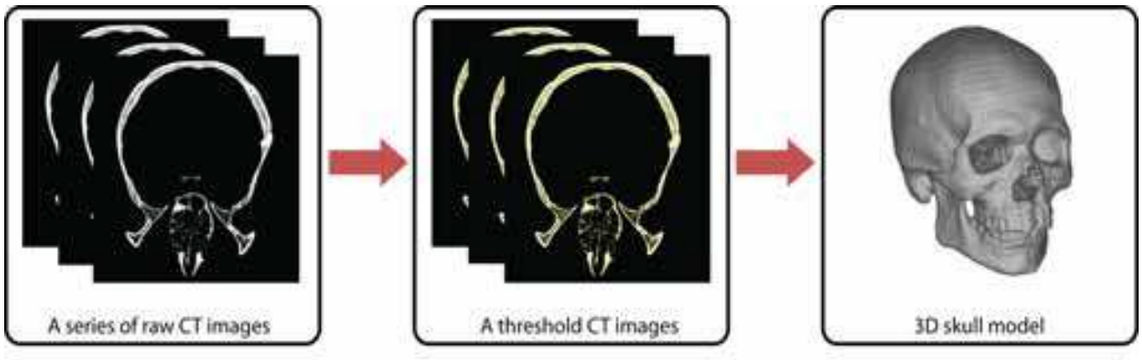

Fig. 4. Three-dimensional model reconstruction.

4. Three-dimensional computerized craniometric study

The anatomical landmarks in craniometric study are categorized in to median and bilateral landmarks (Rooppakhun, et al., 2010). The median landmarks are approximately located on sagittal plane. Each of them has only one location. There are 13 median landmarks which the specific definitions can be described as follows:

- *Glabella (GL)* - the most anterior point of frontal bone between supraorbital in the sagittal plane.
- *Bregma (BR)* - the crossing of the coronal and sagittal sutures on the top of the skull.
- *Opisthocranium (OPC)* - the most posterior point in midline of inion bone which length of the skull is maximum when measure from Galbella point.
- *Nasion (NA)* - the intersection point of the internasal and frontonasal sutures in the sagittal plane.
- *Opistion (OPS)* - the most posterior midsagittal point on the posterior margin of the foramen magnum.
- *Basion (BA)* - the most anterior point of the great foramen magnum in the sagittal plane.
- *Orale (OR)* - the midpoint on the intersection of posterior alveolar sockets rim of the cavities of two upper central incisors.
- *Prosthion (PR)* - the lowest, most anterior point on the alveolar portion of the premaxilla, in the median plane, between the upper central incisors.
- *Staphylion (STA)* - point in the medial line (interpalatal suture) of the posterior part of the hard palate where it is crossed by a line drawn tangent to the curves of the posterior margins of the palate.
- *Nasospinale (NAS)* - the lowest point of lower anterior nasal aperture in mid-sagittal plane.
- *Gnathion (GN)* - The midpoint on the lower border of the mandible in the sagittal plane.
- *Pogonion (PG)* - The most projecting point of the chin in the standard sagittal plane.
- *Infradentale (ID)* - The anterior superior point on the mandible at its labial contact between mandibular central incisors.

For the bilateral landmarks, each of them is located on both sides of skull. There are 17 bilateral landmarks which the specific definitions can be described as follows:

- *Euryon (EU)* - the lateral point on either side of the greatest transverse diameter of the skull.
- *Staphanion (ST)* - the intersection of the superior temporal line and the coronal suture.
- *Frontotemporale (FT)* - the most anterior point on either side of temporal crest of the minimum transverse breadth of frontal bone.
- *Bolton (BO)* - The superior point of the curvature between occipital condyle and posterior margin of foramen magnum.
- *Orbitale (ORB)* - the most inferior point of each infraorbital rim .
- *Ectoconchion (EC)* - the most lateral point on each orbital's margin where a line running parallel to upper orbital border cut the lateral orbital margin.
- *Maxillo-frontale (MF)* - the intersection point on anterior lacrimal crest and fronto-maxillary sutures.
- *Supraorbitale (SOR)* - the most superior point of each superior orbital rim.
- *Zygonion (ZG)* - The most lateral point on the outline of each zygomatic arch.
- *Zygomaxillare (ZM)* - The most interior point on each zygomatico-maxillary sutures.
- *Nasal (NS)* - The most lateral point on each nasal's margin where maximum nasal breadth.
- *Endomolare (ENM)* - the most medial point of internal curvature surface of alveolar ridge corresponding to second molar tooth.
- *Coronion (CO)* - The most superior point on each coroniod process.

- *Condylion superior (CS)* - the most superior point on each mandibular condyle.
- *Conlylion laterale (CDL)* - the most lateral point on each mandibular condyle.
- *Gonion (GO)* - the point at each mandibular angle that is defined by dropping a perpendicular from the intersection point of the tangent lines to the posterior margin of the mandibular vertical ramus and inferior margin of the mandibular body or horizontal ramus.
- *Laterla infradentale (LID)* - the midpoint of a line tangent to the outer margins of the cavities of the lateral incisor of each lower canine teeth.

In order to better understand the previous described definitions, every landmark is also illustrated in Fig. 5.

Each of the three-dimensional models of skull is used to determine the anatomical landmark according to previous description. Only one investigator locate the entire landmarks in every skull to avoid uncertainty of intra-observer. The anatomical landmarks are then used to obtain 40 craniometric parameters as shown in Table 2. The measurements are interpreted using statistical analysis and reported in form of average values and standard deviation regarding to gender. In order to distinguish craniometric parameters of each gender, an unpaired t-test is utilized for analysis. A p-value < 0.05 is a significant level that used to determine the difference. In addition, the linear regression and the correlation coefficient are also used for the pair-wise tests.

As also shown in Table 2, the craniometric parameters of male are larger than female. Thirty-one of forty parameters show the statistical significant differences among both genders, especially, Maximum cranial breadth, Facial length, Orbital height-left, Orbital height-right, Palatal breadth, Bicoronion breadth, Bizygometic breadth, Maxillary breadth, Upper facial height, Orbital breadth-left, Orbital breadth-Right, Nasal height, Bicondylar breath, Bi-gonion breadth, Coronion height-left, Coronion height-right, Mandibular body length-left, Mandibular body length-right, Maximum mandibular length-left and Maximum mandibular length-right which present the p-value $<< 0.001$. For Maximum cranial breadth, Facial length, Orbital height-left, Orbital height-right, Palatal breadth, Bicoronion breadth are considered to be relatively different as the p-value < 0.01. The parameters such Ramus height-left, Ramus height-right, Symphysic height shows some degrees of significance. In addition, nine parameters do not present the statistical differences which are Maximum frontal breadth, Anterior inter-orbital breadth, Nasal breadth, Palatal length, Mandibular angle-left, Mandibular angle-right, Notch length-left, Notch length-right, and Symphysic breadth.

From the pair-wise tests, the correlations of craniometric parameters are different among male and female population. Table 3 and Table 4 show the sample of correlations of craniometric parameters which correlation coefficient (r) are above 0.500. In both populations, the bilateral anatomy presents some degrees of correlation which can be signified the facial symmetry. The linear regression equations are considered to be useful to predict the craniometric parameters in forensic medicine. For example, the defected skull usually miss some landmarks, the use of known craniometric parameters can be used to determine the missing parameters. However, it should be noticed that the obtained missing parameters may not be always precise. The possibility of being can only be determined, but the accuracy strongly depends on the correlation coefficient. The regression scatters plot and 95% interval bands of some pair-wise tests are plotted in Fig. 6 and Fig. 7.

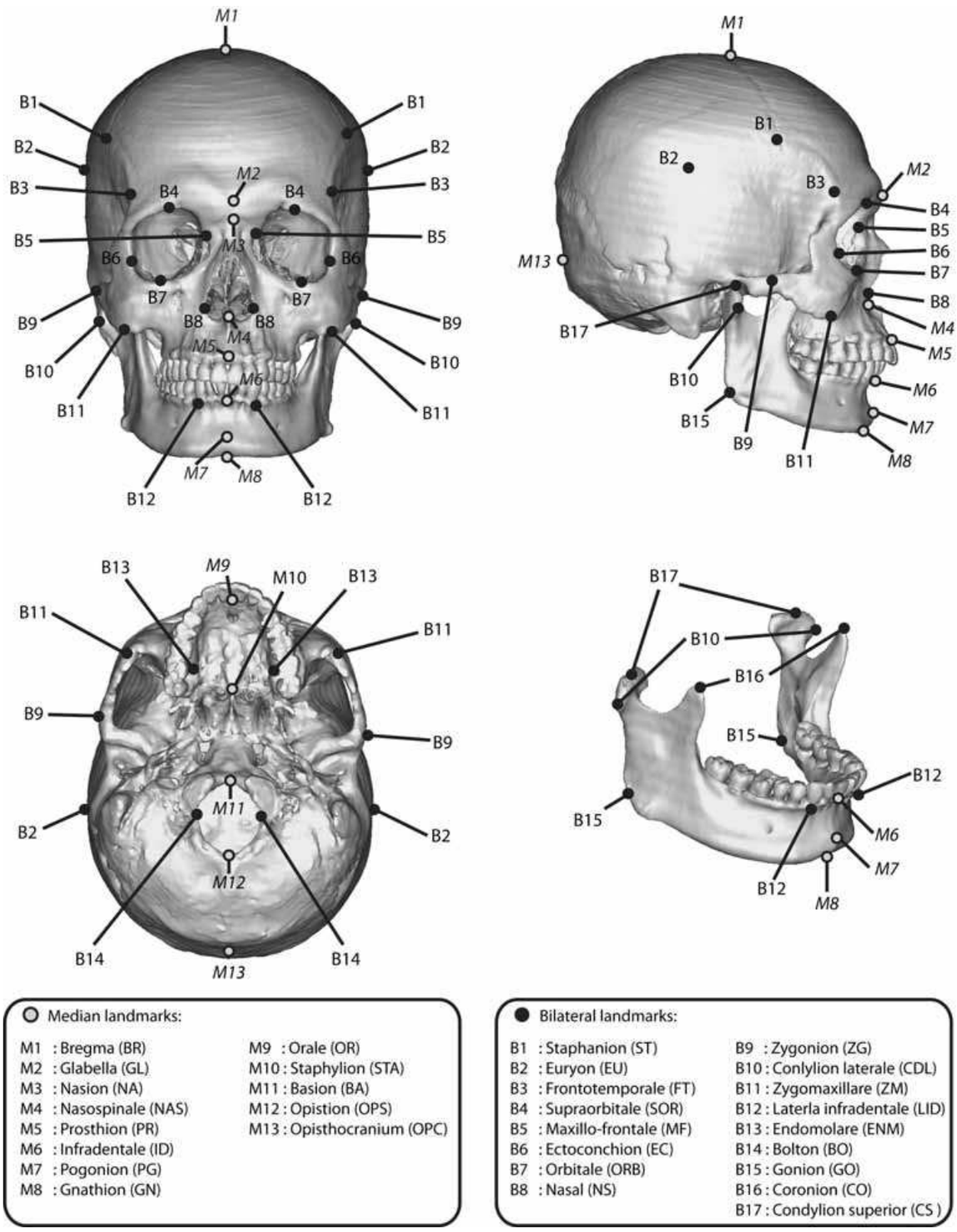

Fig. 5. The anatomical landmarks of skull.

Craniometric Parameter	Landmark	Average (S.D.)		p-value
		Male	Female	
Maximum cranial length	GL-OPC	173.6 (5.2)	165.4 (6.4)	<< 0.001
Maximum cranial breadth	EU_L-EU_R	144.9 (5.6)	141.2 (5.5)	0.001361
Maximum frontal breadth	ST_L -ST_R	115.8 (6.7)	113.3 (6.7)	0.070663
Minimum frontal breadth	FT_L-FT_R	94.9 (5.1)	91.4 (4.9)	0.000584
Basion-brema height	BA-BR	138.6 (4.8)	132.4 (5.2)	<< 0.001
Nasion-basion length	NA-BA	101.8 (4.0)	96.0 (3.4)	<< 0.001
Foramen magnum length	BA-OPC	36.7 (2.1)	34.5 (2.4)	0.000006
Foramen magnum breadth	BO_L-BO_R	30.5 (2.1)	28.9 (1.8)	0.000051
Nasion-bregma length	NA-BR	112.9 (4.2)	107.3 (6.0)	0.000002
Facial length	BA-PR	96.1 (5.4)	92.9 (5.5)	0.004704
Bi-orbital breadth	EC_L-EC_R	97.4 (3.8)	94.0 (3.8)	0.000024
Bi-zygometic breadth	ZG_L-ZG_R	133.7 (5.1)	127.7 (5.2)	<< 0.001
Maxillary breadth	ZM_L–ZM_R	104.5 (5.3)	99.1 (4.9)	0.000001
Upper facial height	NA-PR	70.3 (4.2)	66.2 (4.6)	0.000019
Orbital breadth-left	EC_L-MF_L	41.2 (2.2)	39.6 (2.4)	0.000743
Orbital breadth-right	EC_R-MF_R	41.5 (2.0)	39.8 (2.0)	0.000044
Orbital height-left	ORB_L-SOR_L	36.2 (2.3)	34.7 (2.5)	0.002714
Orbital height-right	ORB_R-SOR_R	36.3 (2.5)	34.9 (2.1)	0.004341
Anterior inter-orbital breadth	MF_L-MF_R	21.0 (2.2)	20.7 (2.4)	0.497642
Nasal breadth	NS_L-NS_R	27.0 (2.2)	26.8 (2.2)	0.632101
Nasal height	NA-NAS	52.7 (3.0)	49.6 (3.1)	0.000003
Palatal length	OR-STA	42.6 (4.2)	42.6 (4.4)	0.952028
Palatal breadth	ENM_L-ENM_R	39.1 (3.1)	37.6 (2.4)	0.006430
Bi-coronion breadth	CO_L-CO_R	98.6 (5.2)	94.3 (5.8)	0.002652
Bi-condylar breadth	CDL_L-CDL_R	123.1 (5.2)	118.7 (5.1)	0.000870
Bi-gonion breadth	GO_L-GO_R	99.1 (6.3)	92.8 (6.2)	0.000113
Coronion height-left	CO_L-GO_L	62.3 (4.9)	57.2 (4.8)	0.000065
Coronion height-right	CO_R-GO_R	62.83 (5.2)	57.5 (4.8)	0.000043
Mandibular angle-left*	CS_L-GO_L-GN	112.4 (5.1)	113.9 (6.4)	0.298443
Mandibular angle-right*	CS_R-GO_R-GN	112.4 (5.5)	112.8 (5.6)	0.759332
Mandibular body length-left	GO_L-PG	92.0 (4.8)	87.0 (4.9)	0.000083
Mandibular body length-right	GO_R-PG	92.5 (4.9)	87.6 (5.0)	0.000128
Maximum mandibular length-left	CS_L-PG	119.8 (6.1)	114.6 (5.1)	0.000383
Maximum mandibular length-right	CS_R-PG	120.6 (6.1)	115.0 (5.0)	0.000079
Notch length-left	CO_L-CS_L	35.3 (2.7)	34.1 (4.2)	0.202213
Notch length-right	CO_R-CS_R	35.1 (2.7)	33.7 (4.0)	0.105663
Ramus height-left	CS_L-GO_L	58.2 (5.0)	55.2 (4.5)	0.010815
Ramus height-right	CS_R-GO_R	58.3 (4.6)	55.3 (4.7)	0.010342
Symphysic breadth	LID_L-LID_R	23.1 (6.0)	23.7 (6.0)	0.689146
Symphysic height	GN-ID	31.6 (3.5)	26.5 (3.1)	0.011128

Table 2. Average values of craniometric parameters regarding to gender derived from 104 skulls (63-males and 41-females), (Unit: millimeter, *degree).

Craniometric Parameter (x vs. y)	Regression (Correlation, r)
Maximum mandibular length-left vs. -right	y = 0.916x + 10.470 (0.920)
Mandibular angle-left vs. -right	y = 0.976x + 2.630 (0.904)
Mandibular body length-left vs. -right	y = 0.883x + 11.227 (0.860)
Coronion height-left vs. -right	y = 0.908x + 6.233 (0.858)
Orbital height-left vs. -right	y = 0.875x + 4.561 (0.835)
Orbital breadth-left vs. -right	y = 0.741x + 10.969 (0.835)
Ramus height-left vs. -right	y = 0.724x + 16.146 (0.835)
Notch length-left vs. -right	y = 0.761x + 8.239 (0.770)
Bi-orbital breadth vs. Orbital breadth-left	y = 0.400x + 2.283 (0.685)
Bi-zygometic breadth vs. Bi-orbital breadth	y = 0.473x + 34.210 (0.643)
Upper facial height vs. Symphysic height	y = 0.485x – 2.733 (0.636)
Maximun cranial breadth vs. Bi-zygometic breadth	y = 0.109x + 17.063 (0.626)
Basion-brema heigth vs. Nasion-bregma length	y = 0.516x + 41.339 (0.594)
Nasal height vs. Upper facial height	y = 0.840x + 25.980 (0.592)
Palatal length vs. Facial length	y = 0.734x + 64.806 (0.570)
Nasion-basion length vs. Bi-coronion breadth	y = 0.730x + 24.429 (0.533)
Bi-condylar breadth vs. Bi-zygometic breadth	y = 0.528x + 67.980 (0.570)

Table 3. The correlation of craniometric parameters of Thai male population.

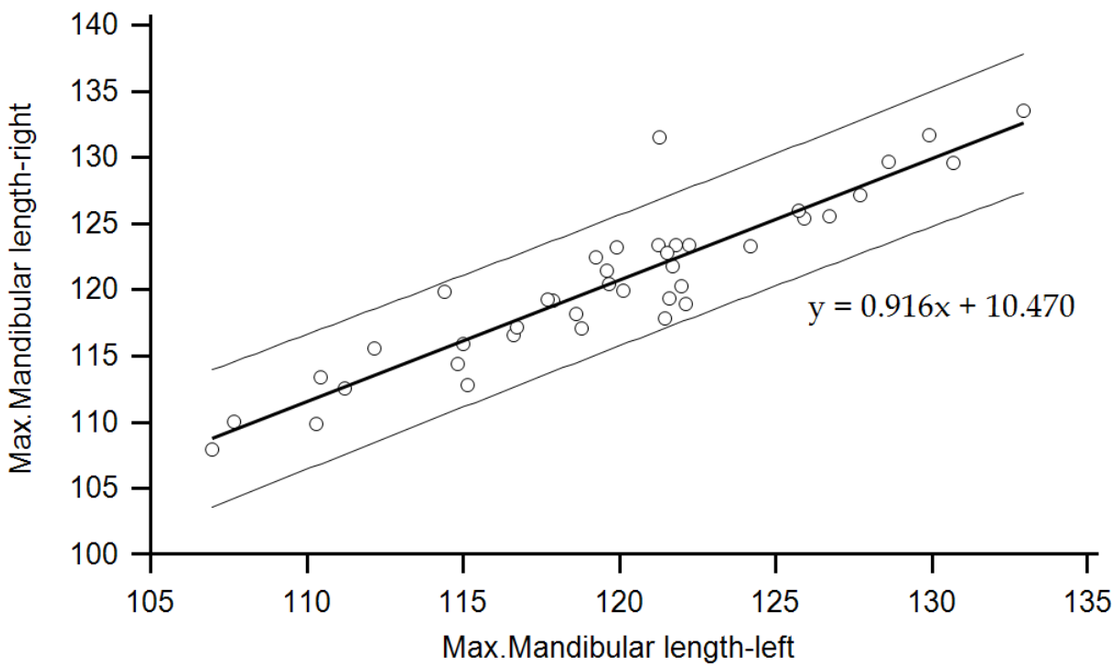

Fig. 6. The linear regression scatters plot and 95% interval bands of Maximum mandibular length-left (x) vs. Maximum mandibular length –right (y) (Unit: Millimeter).

Craniometric Parameter (x vs. y)	Regression (Correlation, r)
Mandibular body length-left vs. -right	y = 0.930x + 6.626 (0.922)
Maximun mandibular length-left vs. -right	y = 0.883x + 13.821 (0.904)
Coronion height-left vs. -right	y = 0.889x + 6.599 (0.895)
Notch length-left vs. -right	y = 0.831x + 5.335 (0.880)
Ramus height-left vs. -right	y = 0.912x + 4.958 (0.871)
Orbital breadth-left vs. -right	y = 0.693x + 12.370 (0.849)
Orbital height-left vs. -right	y = 0.728x + 9.680 (0.839)
Mandibular angle-left vs. -right	y = 0.737x + 28.837 (0.832)
Upper facial height vs. Nasal height	y = 0.522x + 15.065 (0.765)
Bi-orbital breadth vs. Orbital breadth-left	y = 0.478x - 5.357 (0.759)
Minimun frontal breadth vs. Maximum frontal breadth	y = 0.997x + 22.127 (0.723)
Maximun cranial breadth vs. Bi-zygometic breadth	y = 0.624x + 39.615 (0.662)
Symphysic height vs. Upper facial height	y = 0.784x + 42.987 (0.641)
Facial length vs. Palatal length	y = 0.507x - 4.481 (0.637)
Maxillary breadth vs. Bi-orbital breadth	y = 0.474x + 46.949 (0.609)
Anterior interorbital breadth vs. Bi-coronion breadth	y = 1.638x + 60.166 (0.590)
Maximum cranial length vs. Nasion-basion length	y = 0.314x + 43.994 (0.584)

Table 4. The correlation of craniometric parameters of Thai female population.

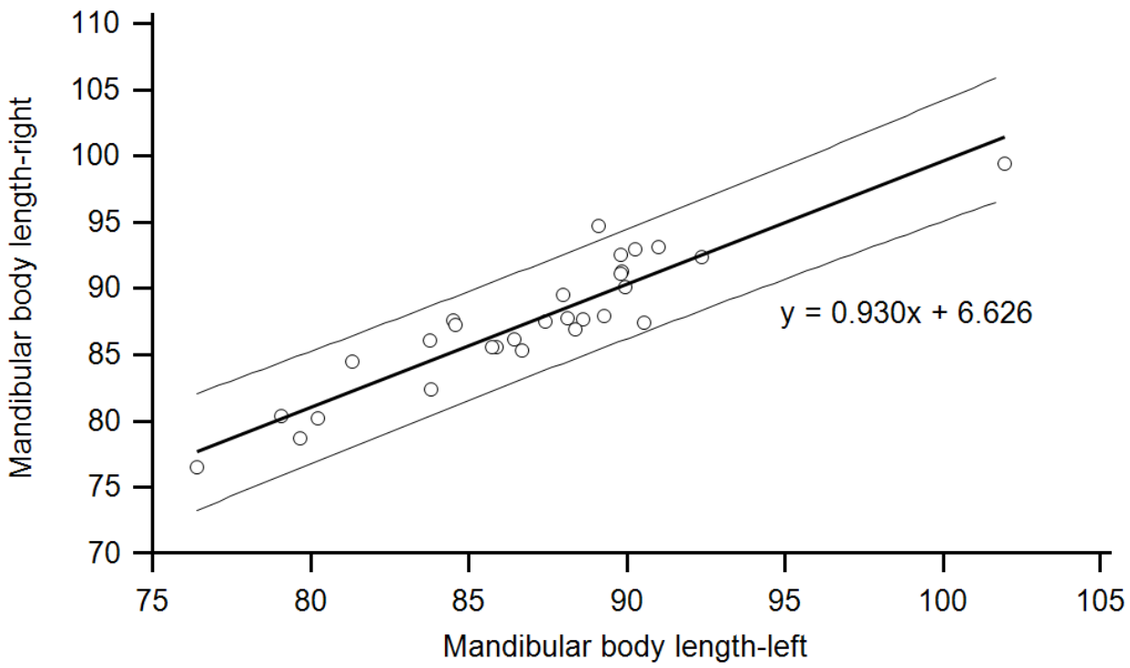

Fig. 7. The linear regression scatters plot and 95% interval bands of Mandibular body length -left (x) vs. Mandibular body length -right (y) (Unit: Millimeter).

5. Sex determination using logistic regression analysis

The determination of sex from skeleton is one of the critical components in forensic medicine as well as archaeology. The determination can be interpreted based on the average data from craniometric parameters of certain population. The accuracy of sex determination depends on several factors which one of them is osteological elements. Various osteological elements have been used to predict sex of skeleton which includes femur (Yaşar Işcan & Shihai, 1995), tibia (Steyn & Işcan, 1997), pelvis (Durić, et al., 2005), skull (King, et al., 1998) , humerus (Işcan, et al., 1998; Robinson & Bidmos, 2009), hyoid (Mukhopadhyay, 2010), talus (Murphy, 2002a) and calcaneus (Murphy, 2002b). However, among aforementioned elements, the best for prediction is pelvis, follow by skull and long bone (Durić, et al., 2005, Işcan, 2005). Rather than osteological element, population variation and method of data processing (data acquisition and statistical analysis) are also among important factors.

Logistic regression analysis is a method to analysis multi-variate analysis which aims to predict the probability of occurrence of an event under consideration by fitting the raw data using to a logit function logistic curve. The advantage of logistic regression is less of parameter restrictions than discriminant analysis and regression analysis. The output from the logistic regression analysis can only be "Yes" or "No" which normally designated as "0" and "1", respectively.

Basically, logistic regression function (Z) is written in form of

$$Z = \beta_0 + \beta_1 x_1 + \beta_2 x_2 + \beta_3 x_3 + \beta_4 x_4 + \ldots + \beta_n x_n + \beta_{n+1} x_{n+1} \quad (1)$$

where β_0 is called intercept and β_1, β_2, β_3 ,β_4, …,β_n and β_{n+1} are regression coefficients of x_1, x_2, x_3, x_4, …,x_n and x_{n+1} variable, respectively. From the following logistic model of Z, the probability of event (P.E.) under consideration can be calculate through

$$P.E. = e^Z / (1 + e^Z) \quad (2)$$

In equation (2) e is a natural logarithm, its value is approximately 2.71828.

The probability of event varies from "0" to "1". The near "1" value means the independent variables influences the probability of event whereas the value close to "0" means the independent variables have little effect to probability of event.

In this study, a binary logistic regression using forward stepwise is applied to determine sex based on average data of craniometric parameters in previous section. The fitting process excludes the measurement with high co-linearity. The probability from logistic regression function, "0" indicates male whereas "1" indicates female, respectively. All statistical analysis is preformed using statistic commercial software (SPSS, SPSSTM Inc, United States of America).

There are three logistic regression models used in sex prediction. ***Model A*** uses only cranial parameters whereas ***Model B*** uses only mandibular parameters. ***Model C*** uses combination of cranial and mandibular parameters. From the analysis, the coefficient (β), standard error of means and significant value are reported as shown in Table 5 to Table 7.

For ***Model A***, there are four significant predictors ($p < 0.05$) in mandible parameters which are Nasion-basion length, Palatal length, Upper facial height and Maxillary breadth. The function is as follows:

Craniometric Parameter	Coefficient (β)	Standard error of mean (S.E.)	Significant level
Intercept	76.340	15.9577	0.00000
Nasion-basion length	-0.387	0.0984	0.00008
Palatal length	0.362	0.1238	0.00349
Upper facial height	-0.497	0.1608	0.00199
Maxillary breadth	-0.197	0.0708	0.00530

Table 5. Logistic response model using logistic regression analysis of *Model A*.

Craniometric Parameter	Coefficient (β)	Standard error of mean (S.E.)	Significant level
Intercept	70.589	18.7774	0.00017
Bi-gonion breadth	-0.184	0.0631	0.00347
Coronion height-left	-0.310	0.1042	0.00289
Mandibular angle-right	-0.208	0.0812	0.01033
Mandibular body length-right	-0.125	0.0888	0.15810

Table 6. Logistic response model using logistic regression analysis of *Model B*.

Craniometric Parameter	Coefficient (β)	Standard error of mean (S.E.)	Significant level
Intercept	88.202	24.4335	0.00031
Coronion height-left	-0.276	0.1242	0.02614
Nasion-basion length	-0.596	0.1741	0.00062
Palatal length	0.581	0.2032	0.00422
Upper facial height	-0.567	0.2186	0.00956

Table 7. Logistic response model using logistic regression analysis of *Model C*.

$$Z = 76.340 - 0.387(\text{NA-BA}) + 0.362(\text{OR-STA}) - 0.497(\text{NA-PR}) - 0.197(ZM_L–ZM_R) \quad (3)$$

where
NA-BA = Nasion-basion length (unit: millimeter)
OR-STA = Palatal length (unit: millimeter)
NA-PR = Upper facial height (unit: millimeter)
$ZM_L–ZM_R$ = Maxillary breadth (unit: millimeter)

For *Model B*, there are four significant predictors ($p < 0.05$) in mandibular parameters which are Bigonion breadth, Coronion height-left, Mandibular angle-right and Mandibular body length-right. The function is as follows:

$$Z = 70.589 - 0.184(GO_L\text{-}GO_R) - 0.310(CO_L\text{-}GO_L) - 0.208(CS_R\text{-}GO_R\text{-GN}) - 0.125(GO_R\text{-PG}) \quad (4)$$

where
GO_L-GO_R = Bi-gonion breadth (unit: millimeter)
CO_L-GO_L = Coronion height-left (unit: millimeter)
CS_R-GO_R-GN = Mandibular angle-right (unit: degree)
GO_R-PG = Mandibular body length-right (unit: millimeter)

For *Model C*, there are four significant predictors in cranial and mandibular parameters ($p < 0.05$) which are Coronion height-left, Nasion-basion length, Palatal length, and Upper facial height. The function is as follows:

$$Z = 88.202 - 0.276(CO_L\text{-}GO_L) - 0.596(\text{NA-BA}) + 0.581\ (\text{OR-STA}) - 0.567\ (\text{NA-PR}) \quad (5)$$

where

CO_L-GO_L = Coronion height-left (unit: millimeter)
NA-BA = Nasion-basion length (unit: millimeter)
OR-STA = Palatal length (unit: millimeter)
NA-PR = Upper facial height (unit: millimeter)

The set of skulls are tested according to logistic regression models (*Model A*, *Model B and Model C*) to evaluate the accuracy as reported in Table 8.

Model	Male	Female	Overall
Model A	92.1	90.2	91.3
Model B	85.0	86.2	85.5
Model C	95.0	93.1	94.2

Table 8. Accuracy of each logistic model (percentage).

The logistic regression analysis revealed that 4 of 21 cranial parameters and 4 of 11 mandibular parameters are significant predictors ($p < 0.05$). The Basion-nasion length and Bigonion breadth are the most dimorphic of the cranial and mandibular measurement, respectively. For the best prediction model, *Model C* which includes both cranial and mandibular parameters is recommended.

In order to predict the gender by the parameters in *Model C*, the probability of being female can be calculated using equation (2) whereas the probability of being male is then inversed (1-P).

The accuracies from *Model C* of the present study are compared to previous studies on sexual dimorphism using the skull of some previous studies based on South African white, South African black, Indian and Thai population. Table 9 shows a comparison of measurement techniques and average accuracies obtained from the present study and previous studies which derived from many populations.

To the best of author's knowledge, there is only one study (Sangvichien, et al., 2007) that determine the sex of skull based on logistic function using on four parameters which as Nasion-basion length, Maximum breadth of the cranium, Facial height, and Bi-zygometic breadth. This presented the accuracy 88.8% for overall sex classification and 82.9% and 92.1% among females and males, respectively.

From the table, it reveals that the present study yields higher accuracies than the many previous studies. Therefore, the *Model C* presents in this study can be used to determine the gender of skeleton for intact skull in forensics and archaeology. However, in order to ensure the effectiveness of logistic regression, three skulls with known gender from Thammasat University Hospital, Thammasat University, Thailand are used to test the concept. The skull No.1 and skull No. 3 are adult males whereas the skull No. 2 is adult female.

Based on logistic regression Model C which is consider to be the best model for sex prediction in Thais' skull , Coronion height-left, nasion-basion length, palatal length, upper facial height are measured and predicted the gender. As shown in Table 10, all cases are predicted the gender correctly (3/3). Hence, the determination of sex based on the Model C of logistic regression is considered to be accurate.

Population	Measurement Technique	Statistical Analysis Method	Average Accuracies
South African White (Steyn & Işcan, 1997) • 44 males • 47 females	Direct measurement	Discriminant function	80% - 86%
South African black (Franklin, et al, 2005) • 182 males • 150 females	3D tactile digitizer	Discriminant function	75% - 80%
Indian (Deshmukh & Devershi, 2006) • 40 males • 34 females	Direct measurement	Discriminant function	85% - 90%
Thai (Sangvichien, et al., 2007) • 66 males • 35 males	Direct measurement	Logistic function	83% - 92%
South African black (Dayal, et al, 2008) • 60 males • 60 males	Direct measurement	Discriminant function	80% - 85%
Combination (Matamala, et al, 2009) • 149 males • 77 males	Direct measurement	Discriminant function	82%
Thai (Present study) • 63 males • 41 males	Three-dimensional CAD Model	Logistic function	93% - 95%

Table 9. Comparison on methods of data assessment and statistical analysis among different studies.

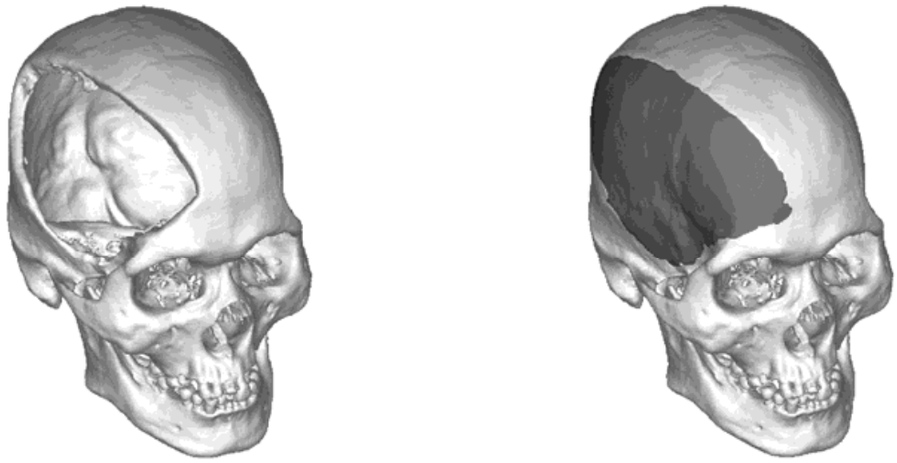

Fig. 8. The reconstruction of skull fragment (A) intact (B) intact with reconstruction unit.

Craniometric Parameter	Skull No.1	Skull No.2	Skull No.3
Intercept	88.202	88.202	88.202
Coronion height-left	69.63	53.12	72.09
Nasion-basion length	105.07	95.24	101.06
Palatal length	58.50	45.82	55.17
Upper facial height	76.91	72.26	71.81
Regression Analysis (Z)	-3.26	2.43	-0.59
Probability of event (P.E.)	0.037	0.919	0.357
Prediction Gender	male	female	male
Exact Gender	male	female	male
Result	correct	correct	correct

Table 10. Craniometric measurement and sex prediction.

6. Outlook

Since there is possibility to find skull as fragment bone in forensics and archaeology, then the assessment of necessary craniometric parameters becomes complex. Although the missing craniometric parameters can be predicted using correlation as shown in Table 3 and Table 4, but some correlation coefficients among these craniometric parameters are mostly inferior. With low correlation coefficient, the equation may not be an appropriate solution to determine those missing craniometric parameters.

As a result, a purposed alternative is to reconstruct defected skull surface based on the mirror surface topology of normal side with aids of Computer Aided Design technique as shown in Fig. 8. In fact, this technique is a standard protocol for implant design in cranial reconstruction (Müller, et al., 2003). The purposed alternative relies on the discovery that the symmetric between left and right of bilateral craniometric parameters as presented in Table 2. However, this concept should be further investigated to ensure the usability.

7. Conclusion

This study presents advantages of using advance medical imaging and reverse engineering through computed tomography scanner to reconstruct the three-dimensional model of skulls. This is very useful to analyze and measure craniometric parameters based on virtual model. Generally, in forensic medicine and archaeological researches, the study relies on direct measurement and other two-dimensional techniques which may not be accurate. The measurement errors can be influenced by human error, instrumental error, image magnification and image occlusion. The advantage of three-dimensional computed tomography technique includes the analysis of specimen without destruction or damage of specimens as well as the ability to analyze the specimens in configuration which the conventional technique cannot provide. Comparing to the other reverse engineering technologies, computed tomography presents the superior ability in accessing the internal geometry which the other tools find the difficulty in data capturing.

In the craniometric analysis, the medians and bilateral landmarks are accessed. From the analysis, the result reveals that Thai male presents the craniometric parameters greater than Thai female, especially, Maximum cranial breadth, Facial length, Orbital height-left, Orbital height-right, Palatal breadth, Bicoronion breadth, Bizygometic breadth, Maxillary breadth, Upper facial height, Orbital breadth-left, Orbital breadth-Right, Nasal height, Bicondylar breath, Bi-gonion breadth, Coronion height-left, Coronion height-right, Mandibular body length-left, Mandibular body length-right, Maximum mandibular length-left and Maximum mandibular length-right. In both populations, the bilateral anatomy presents some degrees of correlation which may be concluded the facial symmetry.

Logistic regression is used to derive functions for sex determination based on average numerical values which obtained from craniometric parameters. Three models are purposed, *Model A* is based on cranial parameters, *Model B* is based on mandible parameters and *Model C* is based on both cranial and mandibular parameters. From the result, *Model C* provides the best accuracy among other models which is 94.2%. The prediction equation relies on four parameters which are Coronion height-left, Nasion-basion length, Palatal length, and Upper facial height which subsequently produce logistic regression as in equation (5).

As seen in Table 9, our study yields higher accuracies than other previous studies. This is due to two main factors, the accurate landmark identification by the three-dimensional technique and developing logistic regression function from difference sample.

In addition, the authors suggest that the techniques described in this chapter which includes data acquisition, three-dimensional computerized craniometric study and sex determination based on logistic regression function can effectively be applied to the other osteological elements in specific race.

8. Acknowledgment

The research is supported the funding and facilities in part by the National Metal and Material Technology Center (MTEC), National Science and Technology Development Agency (NSTDA) of Thailand and Suranaree University of Technology, Thailand. In addition, the authors are grateful to Department of Anatomy, Faculty of Medicine, Khon Kaen University, Thailand for providing cadaveric skull specimens.

9. References

Aamodt, A., Kvistad, K. A., Andersen, E., Lund-Larsen, J., Eine, J., Benum, P. & Husby, O. S. (1999). Determination of the Hounsfield value for CT-based design of custom femoral stems. *JBone Joint Surg [Br]*, Vol. 81(1), pp. 143-147

Aghayev, E., Staub, L., Dirnhofer, R., Ambrose, T., Jackowski, C., Yen, K., Bolliger, S., Christe, A., Roeder, C., Aebi, M. & Thali, M. J. (2008). Virtopsy - The concept of a centralized database in forensic medicine for analysis and comparison of radiological and autopsy data. *JForensic Leg Med*, Vol. 15(3), pp. 135-140

Chantarapanich, N., Sitthiseripratip, K., Mahaisavariya, B., Wongcumchang, M. & Siribodhi, P. (2008). 3D geometrical assessment of femoral curvature: A reverse engineering technique. *JMed Assoc Thai*, Vol.91(9), pp. 1377-1381

Dayal, M. R., Spocter, M. A. & Bidmos, M. A. (2008). An assessment of sex using the skull of black South Africans by discriminant function analysis. *HOMO*, Vol.59(3), pp.209-221

De Valck, E. (2006). Major incident response: Collecting ante-mortem data. *Forensic Sci Int*, Vol. 159(1), pp. S15-S19

Dedouit, F., Géraut, A., Baranov, V., Ludes, B., Rougé, D., Telmon, N. & Crubézy, E. (2010). Virtual and macroscopical studies of mummies-Differences or complementarity? Report of a natural frozen Siberian mummy. *Forensic Sci Int*, Vol. 200(1-3), pp.e7-e13

Deshmukh, A. & Devershi, D. (2006). Comparison of Cranial Sex Determination by Univariate and Multivariate Analysis. *JAnat Soc*, Vol. 55(2), pp. 48-51

Durić, M., Rakočević, Z. & Donić, D. (2005). The reliability of sex determination of skeletons from forensic context in the Balkans. *Forensic Sci Int*, Vol. 147 (2-3 SPEC.ISS.), pp. 159-164

Franklin, D., Freedman, L. & Milne, N. (2005). Sexual dimorphism and discriminant function sexing in indigenous South African crania. *HOMO*, Vol. 55(3), pp. 213-228

Friedrich, K. M., Nemec, S., Czerny, C., Fischer, H., Plischke, S., Gahleitner, A., Viola, T. B., Imhof, H., Seidler, H. & Guillen, S. (2010). The story of 12 Chachapoyan mummies through multidetector computed tomography. *Eur JRadiol*, Vol. 76(2), pp. 143-150

Fürnstahl, P., Székely, G., Gerber, C., Hodler, J., Snedeker, J. G. & Harders, M. (2010). Computer assisted reconstruction of complex proximal humerus fractures for preoperative planning. *Med Image Anal*, doi:10.1016/j.media.2010.07.012

Hill, C. R. (2009). Early days of scanning: Pioneers and sleepwalkers. *Radiography*, Vol. 15(SUPPL.1), pp. e15-e22

Hounsfield, G. N. (1980). Computed medical imaging. *Science*, Vol. 210(4465), pp. 22-28

Işcan, M. Y. (2005). Forensic anthropology of sex and body size. *Forensic Sci Int*, Vol. 147 (2-3 SPEC.ISS.), pp. 107-112

Işcan, M. Y., Loth, S. R., King, C. A., Shihai, D. & Yoshino, M. (1998). Sexual dimorphism in the humerus: A comparative analysis of Chinese, Japanese and Thais. *Forensic Sci Int*, Vol. 98(1-2), pp. 17-29

King, C. A., Işcan, M. Y. & Loth, S. R. (1998). Metric and comparative analysis of sexual dimorphism in the Thai femur. *JForensic Sci*, Vol. 43(5), pp. 954-958

Li, L., Schemenauer, N., Peng, X., Zeng, Y. & Gu, P. (2002). A reverse engineering system for rapid manufacturing of complex objects. *Robot CIM-Int Manuf*, Vol. 18(1), pp. 53-67

Mahaisavariya, B., Sitthiseripratip, K., Oris, P., Chaichanasiri, E. & Suwanprateeb, J. (2004). Fit-and-fill analysis of trochanteric gamma nail for the Thai proximal femur: A virtual simulation study. *JMed Assoc Thai*, Vol. 87(11), pp. 1315-1320

Mahaisavariya, B., Sitthiseripratip, K., Tongdee, T., Bohez, E. L. J., Vander Sloten, J. & Oris, P. (2002). Morphological study of the proximal femur: A new method of

geometrical assessment using 3-dimensional reverse engineering. *Med Eng Phys*, Vol. 24(9), pp. 617-622

Matamala, D. A. Z., Galdames, I. C. S. & Smith, R. L. (2009). Sexual dimorphism determination from the lineal dimensions of skulls. *Int. JMorphol*, 27(1), 133-137

Mukhopadhyay, P. P. (2010). Morphometric features and sexual dimorphism of adult hyoid bone: A population specific study with forensic implications. *J Forensic Leg Med*, Vol. 17(6), pp. 321-324

Müller, A., Krishnan, K. G., Uhl, E. & Mast, G. (2003). The application of rapid prototyping techniques in cranial reconstruction and preoperative planning in neurosurgery. *The Journal of craniofacial surgery*, Vol. 14(6), pp. 899-914

Murphy, A. M. C. (2002b). The talus: Sex assessment of prehistoric New Zealand Polynesian skeletal remains. *Forensic Sci Int*, Vol. 128(3), pp. 155-158

Murphy, A. M. C. (2002a). The calcaneus: Sex assessment of prehistoric New Zealand Polynesian skeletal remains. *Forensic Sci Int*, Vol. 129(3), pp. 205-208

Park, H. K., Chung, J. W. & Kho, H. S. (2006). Use of hand-held laser scanning in the assessment of craniometry. *Forensic Sci Int*, Vol. 160(2-3), pp. 200-206

Recheis, W., Weber, G. W., Schäfer, K., Knapp, R., Seidler, H. & Zur Nedden, D. (1999). Virtual reality and anthropology. *Eur JRadiol*, Vol. 31(2), pp. 88-96

Robinson, M. S. & Bidmos, M. A. (2009). The skull and humerus in the determination of sex: Reliability of discriminant function equations. *Forensic Sci Int*, Vol. 186(1-3), pp. 86.e1-86.e5

Rooppakhun, S., Piyasin, S., Vatanapatimakul, N., Kaewprom, Y. & Sitthiseripratip, K. (2010). Craniometric study of Thai skull based on three-dimensional computed tomography (CT) data. *JMed Assoc Thai*, Vol. 93(1), pp. 90-98

Sangvichien, S., Boonkaew, K., Chuncharunee, A., Komoltri, C., Piyawinitwong, S., Wongsawut, A. & Namwongsa, S. (2007). Sex Determination in Thai Skulls by Using Craniometry: Multiple Logistic Regression Analysis. *Siriraj Med J*, Vol. 59(5), pp. 216-221

Sangvichien, S., Boonkaew, K., Chuncharunee, A., Komoltri, C., Udom, C. & Chandee, T. (2008). Accuracy of Cranial and Mandible Morphological Traits for Sex Determination in Thais. *Siriraj Med J*, Vol. 60(5), pp. 240-243

Sitthiseripratip, K., Van Oosterwyck, H., Vander Sloten, J., Mahaisavariya, B., Bohez, E. L. J., Suwanprateeb, J., Van Audekercke, R. & Oris, P. (2003). Finite element study of trochanteric gamma nail for trochanteric fracture. *Med Eng Phys*, Vol. 25(2), pp. 99-106

Steyn, M. & Işcan, M. Y. (1997). Sex determination from the femur and tibia in South African whites. *Forensic Sci Int*, Vol. 90(1-2), pp. 111-119

Thali, M. J., Braun, M. & Dirnhofer, R. (2003). Optical 3D surface digitizing in forensic medicine: 3D documentation of skin and bone injuries. *Forensic Sci Int*, Vol.137(2-3), pp. 203-208

Van Tiggelen, R. 2004. Ancient Egypt and radiology, a future for the past! *Nucl Instrum Meth B*, Vol. 226(1-2), pp. 10-14

Vanezis, P., Vanezis, M., McCombe, G. & Niblett, T. (2000). Facial reconstruction using 3-D computer graphics. *Forensic Sci Int*, Vol. 108(2), pp. 81-95

Várady, T., Martin, R. R. & Cox, J. (1997). Reverse engineering of geometric models - An introduction. *CAD*, Vol. 29(4), pp. 255-268

Yaşar Işcan, M. & Shihai, D. (1995). Sexual dimorphism in the Chinese femur. *Forensic Sci Int*, Vol. 74(1-2), pp. 79-87

Zhou, X. & Xi, F. (2002). Automated laser scanning system for reverse engineering and inspection. *Int JMach Tool Manu*, Vol. 42(8), pp. 889-897

Zweifel, L., Büni, T. & Rühli, F. J. (2009). Evidence-based palaeopathology: Meta-analysis of PubMed-listed scientific studies on ancient Egyptian mummies. *HOMO*, Vol. 60(5), pp. 405-427

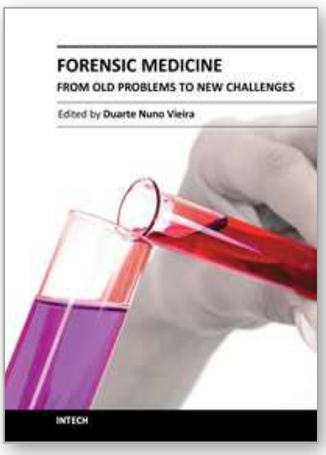

Forensic Medicine - From Old Problems to New Challenges

Edited by Prof. Duarte Nuno Vieira

ISBN 978-953-307-262-3
Hard cover, 382 pages
Publisher InTech
Published online 12, September, 2011
Published in print edition September, 2011

Forensic medicine is a continuously evolving science that is constantly being updated and improved, not only as a result of technological and scientific advances (which bring almost immediate repercussions) but also because of developments in the social and legal spheres. This book contains innovative perspectives and approaches to classic topics and problems in forensic medicine, offering reflections about the potential and limits of emerging areas in forensic expert research; it transmits the experience of some countries in the domain of cutting-edge expert intervention, and shows how research in other fields of knowledge may have very relevant implications for this practice.

InTech Europe
University Campus STeP Ri
Slavka Krautzeka 83/A
51000 Rijeka, Croatia
Phone: +385 (51) 770 447
Fax: +385 (51) 686 166
www.intechopen.com

InTech China
Unit 405, Office Block, Hotel Equatorial Shanghai
No.65, Yan An Road (West), Shanghai, 200040, China
中国上海市延安西路65号上海国际贵都大饭店办公楼405单元
Phone: +86-21-62489820
Fax: +86-21-62489821

IntechOpen